Tapered Cavities for High-Modulation-Efficiency and Low-Distortion Semiconductor Lasers

Farhan Rana, Christina Manolatou, and Martin F. Schubert

***Abstract*—We show that mode structure and cavity geometry in multisegment semiconductor lasers can be tailored to realize high modulation efficiencies as well as low distortion levels in directly modulated semiconductor lasers using the gain-lever effect. Compared with conventional semiconductor gain-lever lasers, the lasers proposed here can have five times higher modulation efficiencies. The second-order harmonic and third-order two-tone intermodulation distortion levels in the proposed lasers are also significantly lower than in conventional gain-lever lasers. We also show that, in the lasers proposed here, unlike in conventional gain-lever lasers, modulation bandwidths and output power levels may not be sacrificed in order to obtain high modulation efficiencies.**

***Index Terms*—Harmonic distortion, intermodulation distortion, laser modulation, semiconductor lasers.**

I. Introduction

DIRECTLY modulated semiconductor lasers are attractive low-cost sources for analog fiber-optic links for applications, such as cable television (CATV) distribution systems, micro-cellular and pico-cellular fiber/coax hybrid links, and phased-arrayed antenna systems [1]–[3]. In conventional semiconductor lasers, each electron (or hole) injected into the device emits at best a single photon and the differential slope efficiency (watts/amps) is limited by $\hbar\omega/e$. The gain of an analog fiber-optic link is proportional to the square of the laser differential slope efficiency and, therefore, a high laser differential-slope efficiency is desirable [1]. Various laser designs have been demonstrated that beat the $\hbar\omega/e$ limit. The slope efficiency of bipolar cascade lasers increases in proportion to the number of cascaded gain sections and can therefore be much in excess of the conventional limit $\hbar\omega/e$. Bipolar cascade lasers with two to three cascaded gain stages have been demonstrated [4]–[7]. The gain in slope efficiency in bipolar cascade lasers comes at the expense of increased device complexity, increased device heating, and increased nonlinearities from the reversed biased Esaki junctions that connect the cascaded gain stages.

Semiconductor gain-lever lasers have also demonstrated large differential slope efficiencies [8], [9]. In a two-segment semiconductor gain-lever laser, the longer segment is heavily forward biased, and only the shorter segment is used for direct current modulation. An increase in the current in the shorter segment increases the carrier density in that segment, causing a large increase in the photon density inside the cavity. The carrier density in the longer segment must decrease so that, in steady state, the round-trip cavity gain equals the cavity loss. The decrease in the carrier density in the longer section comes about as a result of the increased stimulated emission rate due to the increased photon density in the cavity. The large increase in the photon population in the laser cavity results in a large value for the laser differential slope efficiency. Although gain-lever lasers have demonstrated differential slope efficiencies three to five times larger than those of conventional lasers [9], the nonlinearity of the light-versus-current (L–I curve) characteristics of gain-lever lasers results in large signal distortions. In particular, the second-order harmonic distortion (HMD2) and the two-tone third-order intermodulation distortion (IMD3) of gain-lever lasers have been found to be too large for practical applications [10]. In addition, at bias points where the differential slope efficiency is large, the nonlinearities are also large, and the laser output power and the laser modulation bandwidth are both small [10]. An exception to this is the recent results in which optical injection locking was used to increase the modulation bandwidth and reduce the nonlinearities in a gain-lever distributed feedback reflector (DBR) laser at the expense of increased device and system complexity [11]. In particular, a reduction in HMD2 of $\sim$16 dB and a reduction in IMD3 of $\sim$15 dB was reported in [11] without sacrificing the laser modulation bandwidth.

In this paper, we show that the cavity structure in gain-lever semiconductor lasers can be modified to enhance the differential slope efficiency even at large output power levels. We show that this can be achieved together with an increase in the modulation bandwidth and a reduction in the distortion levels. The improvement in the differential slope efficiency compared with conventional gain-lever lasers is related to the device geometry and dimensions and is therefore less sensitive to the dc biasing of the laser. We present cavity designs that have up to three times larger modulation bandwidths, a reduction in HMD2 approaching 20 dB, and a reduction in IMD3 approaching 40 dB, compared with conventional gain-lever lasers for the same modulation efficiency. The laser structures discussed in this paper can lead to cost-effective, high-modulation-efficiency, and low-distortion sources for analog fiber-optic links.

II. Cavity Geomotries for High-Modulation-Efficiency Lasers

In order to illustrate the essential ideas, we consider the two-segment laser cavity shown in Fig. 1. L_1 and L_2 are the lengths

Manuscript received March 27, 2007; revised June 12, 2007. This work was supported by the National Science Foundation under Grant ECS-0636593.

The authors are with the School of Electrical and Computer Engineering, Cornell University, Ithaca, NY 14853 USA (e-mail: fr37@cornell.edu; cm285@cornell.edu; mfs24@cornell.edu).

Color versions of one or more of the figures in this paper are available at http://ieeexplore.ieee.org.

Digital Object Identifier 10.1109/JQE.2007.904461

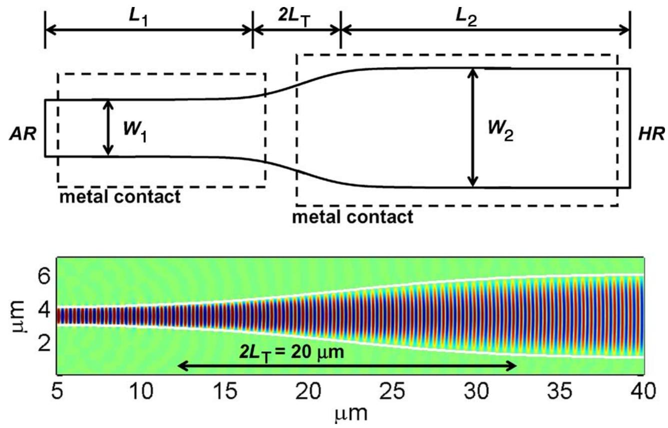

Fig. 1. Top: A two-segment semiconductor laser with different transverse-mode areas in the two segments. Bottom: A 3D-FDTD simulation of a hyperbolic-tangent mode converter connecting fundamental modes of 1- and 5-μm-wide waveguides. More than 96% of the power is transmitted from the fundamental mode in the narrow segment to the fundamental mode in the wide segment and vice versa. Approximately 2% of the incident power is lost to radiation. The power reflected is less than 10^{-3} (both ways).

of the two segments of the laser, A_1 and A_2 are the cross-sectional areas of the active region in the two segments, and Γ_1 and Γ_2 are the transverse-mode gain-confinement factors in the two segments [12]. The transverse-mode effective areas A_{p1} and A_{p2} in the two segments are A_1/Γ_1 and A_2/Γ_2, respectively. Ignoring the tapered section (assuming $2L_T \ll L_1, L_2$), the rate equations for the carrier densities N_1 and N_2 in the two segments, and the average photon density N_p in the laser cavity can be written as

$$\frac{dN_m}{dt} = \eta_i \frac{I_m}{eV_m} - R(N_m) - h_m v_g g_m N_p, \qquad m = 1,2 \quad (1)$$

$$\frac{dN_p}{dt} = \left(\sum_{m=1,2} \Gamma_m \frac{L_m}{L} v_g g_m\right) N_p - \frac{N_p}{\tau_p}. \quad (2)$$

Here, L equals $L_1 + L_2$, the mode effective volume V_p equals $A_{p1}L_1 + A_{p2}L_2$, and the active region volumes V_1 and V_2 of the two segments equal A_1L_1 and A_2L_2, respectively. $R(N_m)$ are the carrier-density-dependent recombination rates. The factors h_m relate the average photon density N_p to the actual photon density in each segment and are given by $h_m = V_p/A_{pm}L$. It is assumed that the narrow segment supports only a single transverse mode which transforms between the narrow and the wide segments of the laser without generating reflections and without exciting higher order transverse modes in the wide segment. The above equations give the following result for the laser differential-slope efficiency:

$$\frac{dP_{\text{out}}}{dI_1} = \left(\eta_o \eta_i \frac{\hbar\omega}{e}\right) \frac{\Gamma_1 g_1 L_1 + \Gamma_2 g_2 L_2}{\Gamma_1 g_1 L_1 + X\Gamma_2 g_2 L_2} \quad (3)$$

where X is given as

$$X = \frac{A_{p1}\tau_2 (dg/dN)_2}{A_{p2}\tau_1 (dg/dN)_1}. \quad (4)$$

Here, η_o is the output coupling efficiency, and τ_1 and τ_2 are the carrier differential recombination lifetimes in the two segments [12]. Note that the first factor in brackets on the right-hand side in (3) is the differential slope efficiency of a conventional laser [12]. The term outside the brackets describes the enhancement due to the gain-lever effect. If $\Gamma_2 g_2 L_2 \gg \Gamma_1 g_1 L_1$ and $X < 1$, the enhancement in the slope efficiency is given by $\sim 1/X$. Compared with a conventional gain-lever laser, the value of X for a laser with different transverse-mode areas in the two segments is reduced by the ratio A_{p1}/A_{p2}. As we show below, the mode areas in the two segments can be made different by factors as large as ten, and therefore the enhancement in the differential-slope efficiency compared to conventional gain-lever lasers can be significant. This enhancement can be traded off for reduced nonlinearity, increased modulation bandwidth, and increased output power.

III. Numerical Simulation Results

For a more detailed analysis, we present numerical simulation results for two-segment lasers having different widths W_1 and W_2 in the two segments (as shown in Fig. 1). We consider a three-quantum-well (70 Å each) InGaAsP–InP active region (1.55-μm wavelength; $L_1 = 100$ μm and $L_2 = 200$ μm). The ratio A_{p2}/A_{p1} of the transverse-mode areas in the two segments approximately equals the ratio W_2/W_1 of the widths of the two segments. A variety of adiabatic as well as nonadiabatic compact mode-converter designs have been reported in the literature [13]. We consider one of the simpler designs and assume that the two segments are joined by a hyperbolic-tangent adiabatic mode converter in which the waveguide width $W(z)$ is given approximately by

$$W(z) = \frac{W_2 + W_1}{2} + \frac{W_2 - W_1}{2} \tanh\left(\frac{z - z_o}{L_T}\right). \quad (5)$$

The location z_o is at the center of the mode converter. More than 75% of the of the width transition occurs in a length $2L_T$. In simulations, the width W_1 of the narrow segment is assumed to be 1 μm and the width W_2 of the wide segment is varied. Losses associated with mode conversion are calculated using three-dimensional finite–difference time–domain (3D-FDTD). Fig. 1 shows the transverse mode for $W_2 = 5$ μm and $L_T = 10$ μm. More than 96% of the power is transmitted from the fundamental mode in the narrow segment to the fundamental mode in the wide segment and vice versa. Approximately 2% of the incident power is lost to radiation. The power reflected is less than 10^{-3} (both ways). For $W_2 = 10$ μm and $L_T = 25$ μm, the power transmitted is more than 89% (both ways), and the power reflected is less than 10^{-3} (both ways). We should emphasize here that the performance parameters of the lasers proposed here, such as modulation efficiency and distortion, are not a sensitive function of the mode-converter design or characteristics as long as the mode converter is relatively compact (i.e., the length of the mode converter is small compared with the total length of the laser), does not introduce excessive losses, and does not generate large reflections. Excessive losses could result in increased threshold current density, increased device

TABLE I
LASER PARAMETER VALUES USED IN SIMULATIONS [12]

Parameter	**Value**
Length L_1, L_2, and L_T	100, 200, and 25 μm, respectively
Gain confinement factors Γ_1 and Γ_2	.04 and .04, respectively
Width W_1	1 μm
Current injection efficiency η_i	0.85
Recombination rate model	$R(N) = AN + BN^2 + CN^3$
Recombination parameter A	5×10^7 1/s
Recombination parameter B	10^{-10} cm^3/s
Recombination parameter C	5×10^{-29} cm^6/s
Gain model	$g = (g_o/(1+\epsilon N_p))\ \ln(N/N_{tr})$
Parameter g_o	1800 1/cm
Transparency density N_{tr}	1.7×10^{18} 1/cm^3
Gain compression factor ϵ	5×10^{-17} cm^3
Waveguide intrinsic loss α_i	10 1/cm
Product of facet reflectivities	0.9×0.1

heating, and reduced modulation efficiency. A longer mode converter would result in a shorter length for the wider segment for the same total laser length, resulting in reduced modulation efficiency (total laser length can be increased but only at the expense of the modulation bandwidth). Our choice for hyperbolic-tangent adiabatic mode converter is dictated more by simplicity than performance. For example, adiabatic parabolic and more sophisticated nonadiabatic mode converters have been reported to achieve more than 95% transmission over only a few micrometers distances between waveguides with width ratios larger than 5 [13]. However, the performance provided by the hyperbolic-tangent mode converter is more than adequate to demonstrate the characteristics of the proposed lasers. The assumed values of the other device parameters are shown in Table I. The device is HR/AR-coated for most of the light to come out of the facet on the side of the narrow segment for better output mode quality. The length L_T for the taper is assumed to be 25 μm. The length of the entire laser structure is $L_1 + L_2 + 2L_T$. Our simulations include the effects of longitudinal as well as transverse spatial hole burning in the rate equations, as in [14]. For every bias point, the photon density is found at every location in the laser cavity (assuming only a single transverse lasing mode), and its value is used to set up time-dependent rate equations for the carrier density at every location in the laser cavity and the average photon density in the laser cavity [14]. These rate equations are used to compute the direct current modulation response of the laser. The carrier-photon dynamics in the tapered section are therefore also included in the analysis. Carrier diffusion effects have been ignored for simplicity.

Fig. 2 shows the calculated output powers and slope efficiencies (normalized to the slope efficiency $\eta_o\eta_i\hbar\omega/e = 0.41$ mW/mA of a conventional single-segment laser of equal length) as a function of the current I_1 in the narrow segment for different values of the width W_2 of the wide segment. The bias current I_2 in the wide segment has values equal to 11, 27.5, 55, and 110 mA for lasers with width W_2 equal to 1, 2.5, 5, and 10 μm, respectively. The current I_2 is chosen such that, when $I_1 = 0$, the gain g_2 provided by the wide segment is as large as possible without causing lasing [8]–[11]. Fig. 2 shows that the slope efficiency of the laser increases with the ratio W_2/W_1. In a conventional gain-lever laser, $W_2 = W_1$, and the slope efficiency enhancement occurs only for small values of the current I_1 and the output power. When the ratio W_2/W_1 is large, the slope efficiency is large even for large values of the current I_1 and the output power. In a conventional gain-lever laser, at small bias current values for which the slope efficiency is large, the rate of change of the slope efficiency with the bias current is also large. Thus, slope efficiency enhancement comes at the expense of increased nonlinearity and reduced dynamic range for RF modulation. However, when W_2/W_1 is large, the laser can be biased well above threshold where the slope

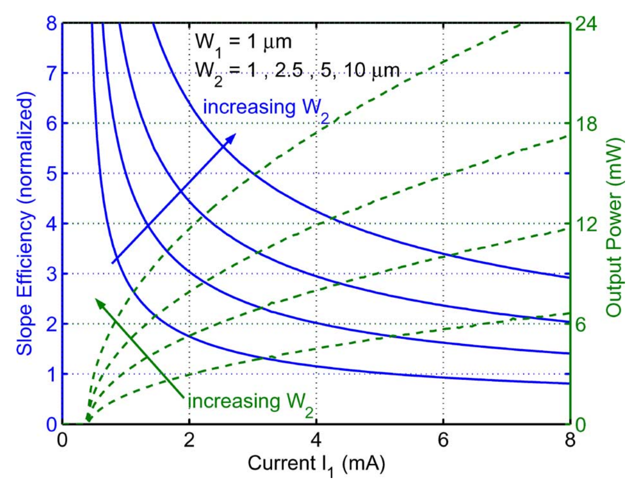

Fig. 2. Slope efficiencies (solid line) and output powers (dashed line) are plotted as a function of the current I_1 in the narrow segment for different widths W_2 of the wide segment. The bias currents I_2 in the wide segment for widths 1.0, 2.5, 5.0, and 10 μm are 11, 27.5, 55, and 110 mA, respectively. The slope efficiencies are normalized to the slope efficiency $\eta_o\eta_i\hbar\omega/e$ of a conventional single-segment laser of equal length. Values of the device parameters are shown in Table I.

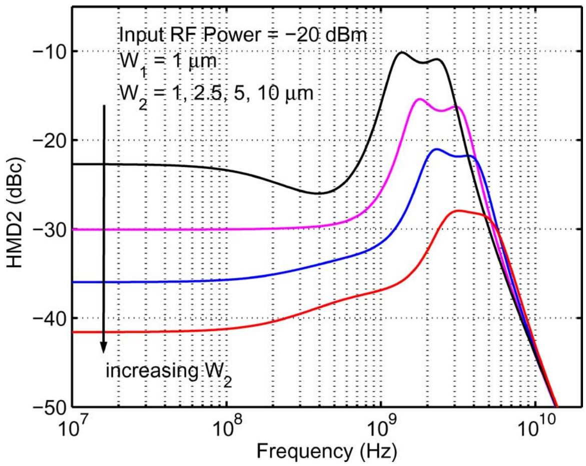

Fig. 3. HMD2 normalized to the fundamental is plotted as a function of the frequency of the fundamental for different values of the width W_2 of the wide segment. The bias currents I_2 in the wide segment for widths 1.0, 2.5, 5.0, and 10 μm are 11, 27.5, 55, and 110 mA, respectively. The bias currents I_1 are such that the differential slope efficiency of each laser structure is three times that of a conventional single-segment laser of equal total length. Values of the device parameters are shown in Table I.

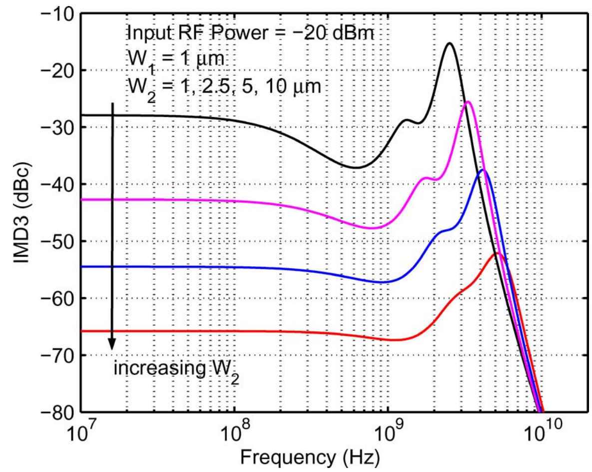

Fig. 4. The two-tone IMD3 normalized to the fundamental is plotted as a function of the frequency of the carrier for different values of the width W_2 of the wide segment. The frequencies f_1 and f_2 of the input signals are assumed to be centered around the carrier frequency and separated by 1 MHz. The distortion product at $2f_2 - f_1$ is calculated for IMD3. The bias currents I_2 in the wide segment for widths 1.0, 2.5, 5.0, and 10 μm are 11, 27.5, 55, and 110 mA, respectively. The bias currents I_1 are such that the differential slope efficiency of each laser structure is 3 times that of a conventional single-segment laser of equal total length. Values of the device parameters are shown in Table I.

efficiency is still relatively large but the nonlinearity is small and the dynamic range is large. The enhancement of the slope efficiency with the ratio W_2/W_1 can be explained as follows. When the current I_1 in the narrow segment increases, the carrier density in that segment also increases. Since the round-trip gain is fixed above threshold and equals the round-trip cavity loss, the gain, and therefore the carrier density, in the wide segment must decrease. This decrease comes about as a result of an increase in the photon generation rate through stimulated emission. If the width W_2 is large, then the rate generation of photons will also be large so as to achieve the desired reduction in the carrier density.

IV. Modulation Distortion Products (HMD2 and IMD3)

Here, we show that high modulation efficiencies obtained through tapered cavity designs can be sacrificed a little to achieve increased modulation bandwidths and reduced distortions. In order to compare the high-frequency performance and distortion levels in laser structures with different widths W_2 of the wide segment, we assume that each laser structure is biased such that its differential slope efficiency is three times that of a conventional single-segment laser. Under this assumption, the 3-dB modulation bandwidths are approximately 3.3, 5, 7, and 9.5 GHz for lasers with W_2 values equal to 1, 2.5, 5, and 10 μm, respectively. Therefore, larger values of the ratio W_2/W_1 enable larger modulation bandwidths for the same slope efficiency enhancement. HMD2 and two-tone IMD3 are calculated from the rate equations using the standard methods [1], [14]. For IMD3 calculations, we assume an RF input consisting of two frequencies f_1 and f_2 centered at the carrier frequency and separated by 1 MHz. The intermodulation distortion product at $2f_2 - f_1$ is evaluated. The RF power for each input frequency is assumed to be -20 dBm. Fig. 3 shows HMD2 (normalized to the fundamental) as a function of frequency for different values of the width W_2 of the wide segment. It can be seen that HMD2 is reduced by about 20 dB at 1 GHz when the ratio W_2/W_1 is increased from 1 to 10. Fig. 4 shows IMD3 (normalized to the fundamental) as a function of frequency for different values of the width W_2 of the wide segment. Fig. 4 shows that IMD3 is also reduced by approximately 35 dB at 1 GHz when the ratio W_2/W_1 is increased from 1 to 10. The distortion products are seen to have constant frequency-independent values at small frequencies. This is due to the intrinsic nonlinearity of the gain-lever effect which dominates over nonlinearities due to spatial hole burning. In simulations, the value of the gain compression factor ϵ was assumed to be 5×10^{-17} cm^3 [12], [14]. However, gain compression was found to have negligible effect on the HMD2 and IMD3 values shown in Figs. 3 and 4.

It needs to be pointed out here that the value of the parameter X in (3) increases with the bias current I_1 and can even become greater than unity. When this happens, the slope efficiency of the laser becomes less than that of a conventional single-segment laser. This can be seen to happen for the case $W_2/W_1 = 1$ in Fig. 2 for $I_1 > 5.5$ mA. However, the values of I_1 for which X becomes unity increase with the value of the ratio W_2/W_1. Consequently, larger values of the ratio W_2/W_1 allow a wider range of bias values over which the slope efficiency is enhanced. It should be noted here that the specific example of the tapered two-segment laser structure considered here is not the only design by which the transverse-mode areas in the two segments of the laser can be made different. For example, vertical mode converters, reported in [15], can be used to change the mode-confinement factors in the two segments while keeping the same active area, and the ratio A_{p1}/A_{p2} of the transverse-mode areas would then equal the ratio Γ_2/Γ_1 of the mode-confinement factors.

Finally, it needs to be mentioned here that, at very large values of I_1 and output power, device heating, multitransverse-mode lasing, and other nonidealities could become important, and the analysis presented in this paper may not be adequate. Similarly, the maximum achievable values of the ratio W_2/W_1 could be limited by factors, such as device heating and multitransverse-mode lasing, that have not been considered in this paper.

V. Conclusion

We have presented a method to increase the differential slope efficiency of semiconductor gain-lever lasers via modification of the cavity geometry. Our designs allow gain-lever lasers to achieve high slope efficiency, low nonlinearity, large modulation bandwidth, and large output power all at the same time. The ideas presented in this paper could allow cost-effective high-modulation-efficiency laser sources for analog fiber-optic and fiber/coax hybrid communication links.

References

[1] C. H. Cox, *Analog Optical Links: Theory and Practice*. New York: Cambridge Univ. Press, 2004.

[2] W. I. Way, *Broadband Hybrid Fiber/Coax Access System Technologies*. New York: Academic, 1997.

[3] W. S. C. Chang, *RF Photonic Technology in Optical Fiber Links*. New York: Cambridge Univ. Press, 2002.

[4] J. P. van der Ziel and W. T. Tsang, "Integrated multi-layer GaAs lasers separated by tunnel junctions," *App. Phys. Lett.*, vol. 41, no. 6, pp. 499–501, 1982.

[5] J. C. Garcia, E. Rosencher, P. Collot, N. Luarent, J. Guyaux, B. Vinter, and J. Nagle, "Epitaxially stacked lasers with Esaki junctions: A bipolar cascade laser," *Appl. Phys. Lett.*, vol. 71, no. 26, pp. 3752–3754, 1997.

[6] S. G. Patterson, G. S. Petrich, R. J. Ram, and L. A. Kolodzjieski, "Room temperature, continuous wave operation of a bipolar quantum cascade laser," *Electron. Lett.*, vol. 35, no. 5, pp. 395–397, 1999.

[7] J. K. Kim, E. Hall, and L. A. Coldren, "Epitaxially-stacked multiple-active-region 1.55 μm lasers for increased differential efficiency," *Appl. Phys. Lett.*, vol. 74, p. 3251, 1999.

[8] K. J. Vahala and M. A. Newkirk, "The optical gain-lever: A novel gain mechanism in the direct modulation of quantum well semiconductor lasers," *Appl. Phys. Lett.*, vol. 54, pp. 2506–2508, 1989.

[9] N. Moore and K. Y. Lau, "Ultrahigh efficiency microwave signal transmission using tandem-contact single quantum well GaAlAs lasers," *Appl. Phys. Lett.*, vol. 55, pp. 936–938, 1989.

[10] L. D. Westbrook and C. P. Seltzer, "Reduced intermodulation free dynamic range in gain-lever lasers," *Electron. Lett.*, vol. 29, pp. 488–489, 1993.

[11] H. K. Sung, T. Jung, D. Tishinin, K. Y. Liou, W. T. Tsang, and M. C. Wu, "Optical injection-locked gain-lever distributed bragg reflector lasers with enhanced RF performance," in *Proc. IEEE Int. Top. Meet. Microw. Photon.*, 2004, pp. 225–228.

[12] L. A. Coldren and S. Corzine, *Diode Lasers and Photonic Integrated Circuits*. New York: Wiley, 1995.

[13] B. Luyssaert, P. Bienstman, P. Vandersteegen, P. Dumon, and R. Baets, "Efficient nonadiabatic planar waveguide tapers," *J. Lightw. Technol.*, vol. 23, no. 12, pp. 2462–2468, Dec. 2005.

[14] J. Chen, R. J. Ram, and R. Helkey, "Linearity and third-order intermodulation distortion in DFB semiconductor lasers," *IEEE J. Quantum Electron.*, vol. 35, no. 10, pp. 1231–1237, Oct. 1999.

[15] N. Yoshimoto, K. Kawano, H. Takeuchi, S. Kondo, and Y. Noguchi, "Highly efficient coupling semiconductor spot-size converter with an InP/InAlAs multiple-quantum-well core," *J. Appl. Opt.*, vol. 34, pp. 1007–1014, 1995.

Farhan Rana received the B.S., M.S., and Ph.D. degrees from the Massachusetts Institute of Technology (MIT), Cambridge, all in electrical engineering.

He was involved with a variety of different topics related to semiconductor optoelectronics, quantum optics, and mesoscopic physics during his doctoral research. Before starting his doctoral work, he was with IBM's T. J. Watson Research Center, where he was involved with silicon nanocrystal and quantum-dot memory devices. He joined the faculty of the School of Electrical and Computer Engineering, Cornell University, Ithaca, NY, in 2003. His current research focuses on semiconductor optoelctronics and terahertz devices.

Dr. Rana was is the recipient of the National Science Foundation Faculty CAREER Award in 2004.

Christina Manolatou was born in Athens, Greece. She received the Ph.D. degree from the Massachusetts Institute of TechnolSgy (MIT), Cambridge, in 2001, focusing on theoretical analysis and numerical modeling of integrated optical structures.

After a postdoctoral position at MIT, she joined Cornell University, Ithaca, NY, as a Visiting Scientist. She is the author of the book *Passive Components for Dense Optical Integration* (Kluwer, 2001).

Martin F. Schubert was born in Stuttgard, Germany. He received the B.S. and M.Eng. degrees in electrical and computer engineering from Cornell University, Ithaca, NY. He is currently working toward the Ph.D. degree in electrical engineering at Rensselaer Polytechnic Institute, Troy, NY.